AMERICAN SOCIETY FOR MICROBIOLOGY | mBio®

RESEARCH ARTICLE
Host-Microbe Biology

Pulmonary Iron Limitation Induced by Exogenous Type I IFN Protects Mice from *Cryptococcus gattii* Independently of T Cells

Michael J. Davis,[a] Shannon Moyer,[a] Elizabeth S. Hoke,[a] Edward Sionov,[a,b] Katrin D. Mayer-Barber,[c] Dan L. Barber,[d] Hongyi Cai,[e] Lisa Jenkins,[f] Peter J. Walter,[e] Yun C. Chang,[a] Kyung J. Kwon-Chung[a]

[a]Molecular Microbiology Section, Laboratory of Clinical Immunology and Microbiology, National Institute of Allergy and Infectious Diseases (NIAID), National Institutes of Health (NIH), Bethesda, Maryland, USA

[b]Department of Food Quality and Safety, Institute for Postharvest and Food Sciences, Agricultural Research Organization, The Volcani Center, Bet Dagan, Israel

[c]Inflammation & Innate Immunity Unit, Laboratory of Clinical Immunology and Microbiology, National Institute of Allergy and Infectious Diseases (NIAID), National Institutes of Health (NIH), Bethesda, Maryland, USA

[d]T-Lymphocyte Biology Unit, Laboratory of Parasitic Diseases, National Institute of Allergy and Infectious Diseases (NIAID), National Institutes of Health (NIH), Bethesda, Maryland, USA

[e]Clinical Mass Spectrometry Core, National Institute of Diabetes and Digestive and Kidney Diseases (NIDDK), National Institutes of Health (NIH), Bethesda, Maryland, USA

[f]Transport Biochemistry Section, Laboratory of Cell Biology, National Cancer Institute (NCI), Bethesda, Maryland, USA

ABSTRACT *Cryptococcus neoformans* causes deadly mycosis primarily in AIDS patients, whereas *Cryptococcus gattii* infects mostly non-HIV patients, even in regions with high burdens of HIV/AIDS and an established environmental presence of *C. gattii*. As HIV induces type I IFN (t1IFN), we hypothesized that t1IFN would differentially affect the outcome of *C. neoformans* and *C. gattii* infections. Exogenous t1IFN induction using stabilized poly(I·C) (pICLC) improved murine outcomes in either cryptococcal infection. In *C. neoformans*-infected mice, pICLC activity was associated with *C. neoformans* containment and classical Th1 immunity. In contrast, pICLC activity against *C. gattii* did not require any immune factors previously associated with *C. neoformans* immunity: T, B, and NK cells, IFN-γ, and macrophages were all dispensable. Interestingly, *C. gattii* pICLC activity depended on β-2-microglobulin, which impacts iron levels among other functions. Iron supplementation reversed pICLC activity, suggesting *C. gattii* pICLC activity requires iron limitation. Also, pICLC induced a set of iron control proteins, some of which were directly inhibitory to cryptococcus *in vitro*, suggesting t1IFN regulates iron availability in the pulmonary air space fluids. Thus, exogenous induction of t1IFN significantly improves the outcome of murine infection by *C. gattii* and *C. neoformans* but by distinct mechanisms; the *C. gattii* effect was mediated by iron limitation, while the effect on *C. neoformans* infection was through induction of classical T-cell-dependent immunity. Together this difference in types of T-cell-dependent t1IFN immunity for different *Cryptococcus* species suggests a possible mechanism by which HIV infection may select against *C. gattii* but not *C. neoformans*.

IMPORTANCE *Cryptococcus neoformans* and *Cryptococcus gattii* cause fatal infection in immunodeficient and immunocompetent individuals. While these fungi are sibling species, *C. gattii* infects very few AIDS patients, while *C. neoformans* infection is an AIDS-defining illness, suggesting that the host response to HIV selects *C. neoformans* over *C. gattii*. We used a viral mimic molecule (pICLC) to stimulate the immune response, and pICLC treatment improved mouse outcomes from both species. pICLC-induced action against *C. neoformans* was due to activation of well-defined immune pathways known to deter *C. neoformans*, whereas these immune pathways were dispensable for pICLC treatment of *C. gattii*. Since these immune pathways are eventu-

Citation Davis MJ, Moyer S, Hoke ES, Sionov E, Mayer-Barber KD, Barber DL, Cai H, Jenkins L, Walter PJ, Chang YC, Kwon-Chung KJ. 2019. Pulmonary iron limitation induced by exogenous type I IFN protects mice from *Cryptococcus gattii* independently of T cells. mBio 10:e00799-19. https://doi.org/10.1128/mBio.00799-19.

Editor James W. Kronstad, University of British Columbia

Address correspondence to Kyung J. Kwon-Chung, JKCHUNG@niaid.nih.gov.

Received 28 March 2019
Accepted 9 May 2019
Published 18 June 2019

ally destroyed by HIV/AIDS, our data help explain why the antiviral immune response in AIDS patients is unable to control *C. neoformans* infection but is protective against *C. gattii*. Furthermore, pICLC induced tighter control of iron in the lungs of mice, which inhibited *C. gattii*, thus suggesting an entirely new mode of nutritional immunity activated by viral signals.

KEYWORDS *Cryptococcus gattii*, *Cryptococcus neoformans*, HIV, MDA-5, interferons, iron

Cryptococcosis is a deadly mycosis affecting mostly immunocompromised individuals caused by infection by one of two species complexes: *Cryptococcus neoformans* or *Cryptococcus gattii* (1). Both species are widely found in the environment, with most *C. neoformans* isolates associated with avian guano (2, 3) and *C. gattii* isolates mostly arboreal (4, 5). When the infectious agents are species typed, *C. neoformans* versus *C. gattii* infection rates are similar in non-AIDS patients (6). In contrast, AIDS-associated cryptococcosis is mostly caused by *C. neoformans*, despite evidence for similar environmental availability of *C. neoformans* versus *C. gattii* (6). In fact, most modern AIDS (7) and AIDS-associated cryptococcosis cases are in tropical areas where *C. gattii* is enriched, but even in these areas, the clinical imbalance of *C. neoformans* versus *C. gattii* remains (1, 6, 8). Thus, we posited that some aspect of HIV host infection selects *C. neoformans* over *C. gattii*.

Type I interferon (t1IFN) is a family of cytokines initially studied for their induction during viral infection. Indeed, HIV infection induces high t1IFN (9–11). Initial studies described t1IFN induction of antiviral activities (12, 13); however, more recent studies showed that t1IFN impacts nonviral infectious settings (14). Previous work in our group showed that exogenous induction of t1IFN improved host outcomes against several *Aspergillus* species (15) and against *C. neoformans* (16). t1IFN signaling leads to coordinated regulation in hundreds of IFN-responsive genes, but only a small fraction of these have been characterized (17). Additionally, t1IFN-mediated resistance mechanisms to nonviral pathogens remain only partially characterized.

Protective immune responses to cryptococcal infections are thought to require classical type I immunity. These protective responses redirect the Th2 polarization induced by virulent *Cryptococcus* toward Th1 polarization (18–21). In the lungs, Th1 cells secrete IFN-γ and other factors that recruit and activate effector macrophages to become fungicidal (22–26). *In vitro* polarized M1 macrophages and macrophages harvested from resistant hosts are cryptocidal, whereas *in vitro* polarized M2 macrophages are permissive (27–33). Additionally, Th2 T-cell induced M2 polarization may itself be detrimental to the host (34–38). While the pathway or pathways that underlie the balance between cryptococcus-supportive Th2 induction and host-protective Th1 induction remain incompletely characterized, the importance of this balance is well established (39, 40).

Our previous work showed that exogenous induction of t1IFN by administration of poly(I·C) condensed with poly-L-lysine and carboxylcellulose (pICLC), a mimetic of viral double-stranded RNA, improved survival and fungal load of *C. neoformans*-infected mice and that improvement was mediated by classical T helper cell- and IFN-γ-mediated immunity (16). There pICLC reduced T-cell expression of interleukin-4 (IL-4) and IL-5 (Th2 cytokines) and increased tumor necrosis factor alpha (TNF-α), IFN-γ (Th1), and IL-17a (Th17). pICLC also reduced eosinophilia and increased recruitment of monocyte-derived macrophages. Interference with CD4 T cells, IFN-γ, and IL-17a reversed pICLC-mediated resistance to *C. neoformans*, consistent with classical Th1 or Th17 immune patterning mediating pICLC *C. neoformans* resistance (16).

Thus, the goal of this follow-up study was 2-fold: first, to determine if induction of t1IFN could be selecting against *C. gattii* in a mouse model simulating AIDS-associated cryptococcosis and, second, to determine if pICLC-mediated resistance against *C. gattii* is mediated by induction of classical Th1- and IFN-γ-mediated immunity. We approximated the AIDS patient by inducing t1IFN using pICLC and by depleting T cells using

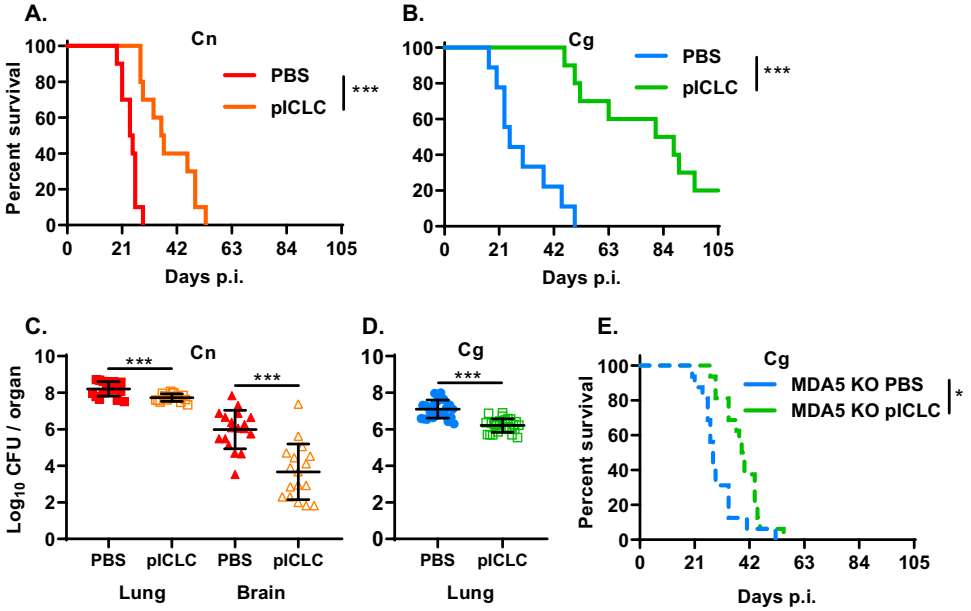

FIG 1 pICLC treatment improves host outcomes in mouse models of cryptococcosis. (A and B) Survival of C57/BL6 mice infected with *C. neoformans* (A [Cn]) or *C. gattii* (B [Cg]) and treated with pICLC or PBS vehicle control twice a week for the duration of the experiment. Data are from a total of 10 mice per group with 2 independent infections. (C and D) Fungal burdens from indicated organs harvested 21 days postinfection with *C. neoformans* (C) or *C. gattii* (D) and treated with pICLC or PBS vehicle control. Data are from 17 to 18 mice per group over 5 independent experiments (C) or 26 mice per group over 8 independent experiments (D). PBS control- versus pICLC-treated groups were compared using Student's *t* test. (E) Survival curves of *C. gattii*-infected MDA-5-deficent mice treated with pICLC or PBS vehicle control. Data are from a total of 15 mice per group with 3 independent infections.

genetic and monoclonal antibody depletion models. With either T-cell depletion technique, the mice depleted of T cells and treated with pICLC displayed equally effective resistance to *C. gattii* infection compared to pICLC-treated mice with intact T-cell compartments. These data contrast with *C. neoformans*-infected mice, which lose pICLC-mediated resistance when T cells are depleted. Thus, our data demonstrate that t1IFN induced by viral infection may select against *C. gattii* and not *C. neoformans* when CD4 T-cell counts are very low in AIDS patients. These data coupled with those showing that IFN-γ and CCR2 were dispensable for pICLC-mediated resistance from *C. gattii* indicated that induction of Th1 immunity was unlikely to mediate this pICLC effect. Instead we present evidence that pICLC-mediated resistance from *C. gattii* is mediated by the induction of iron restriction in the lung air spaces.

RESULTS

PICLC treatment results in better murine outcomes from *C. gattii* or *C. neoformans* infection. As was previously observed (16), pICLC treatment improved survival and fungal burden against cryptococcosis caused by either species. In *C. neoformans*-infected mice, pICLC treatment resulted in an approximately 10-day survival advantage (Fig. 1A), while in *C. gattii*-infected mice, pICLC treatment resulted in a marked 60-day survival advantage (Fig. 1B). These survival advantages were reflected in fungal loads as pICLC modestly reduced lung *C. neoformans* fungal loads but profoundly reduced brain *C. neoformans* fungal loads (Fig. 1C), consistent with our previous report (16). *C. gattii* lung fungal loads were more significantly reduced by pICLC treatment (Fig. 1D). Unlike *C. neoformans* infection, *C. gattii* does not accumulate in the brain (16). Melanoma differentiation-associated protein-5 (MDA-5), a cytosolic sensor protein for double-stranded RNA, was shown to be the major mediator of pICLC effects for *C. neoformans* (16). pICLC treatment of MDA-5-deficient mice showed drastically reduced survival of *C. gattii* infection (Fig. 1E), confirming that pICLC activity in this model results specifically from pICLC–MDA-5 signaling.

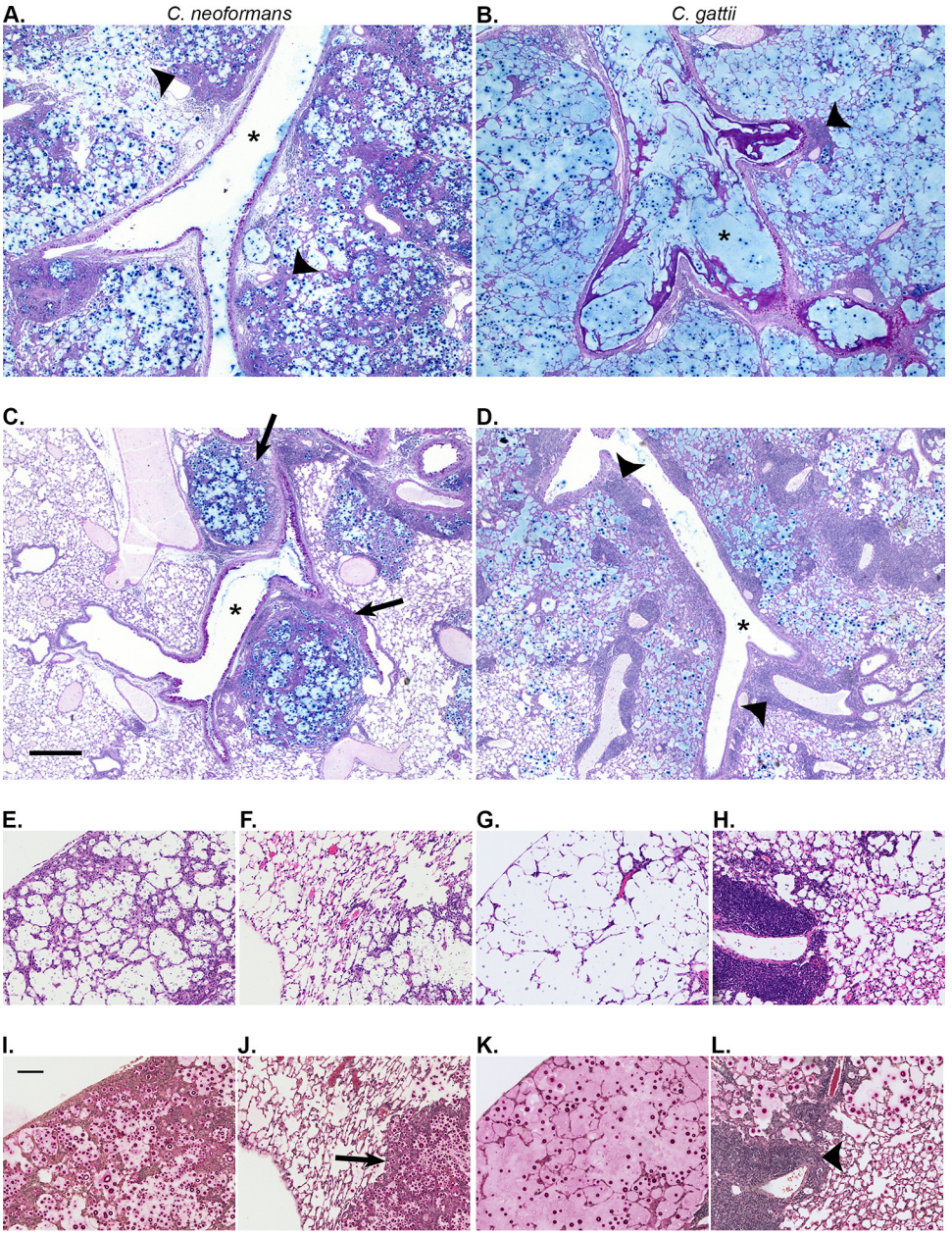

FIG 2 Histopathological examination of infected mice. Lungs were isolated from infected mice at 21 days postinfection. Panels to the left are from *C. neoformans*-infected mice, and those on the right are from *C. gattii*-infected animals. Panels A, B, E, G, I, and K are from PBS-treated animals, while panels C, D, F, H, J, and L are from pICLC-treated animals. Sections pictured in panels A to D were stained with alcian blue (which stains acidic carbohydrates), PAS (which stains neutral carbohydrates), and hematoxylin. Images in panels A to D were acquired using a 2.5× lens objective such that the scale bar in panel B represents 400 μm. Sections pictured in panels E to H were stained with hematoxylin and eosin, while those in panels I and J were stained with mucicarmine and counterstained with hematoxylin. Images in panels E to L were acquired using a 10× lens objective, and the scale bar in panel I represents 100 μm. * marks examples of airways, tailless arrowheads point toward example areas of leukocyte accumulation without apparent yeast containments, tailed arrows point toward example areas of leukocyte accumulation with containment of infection, and "x" marks an example of alveolar destruction in panel G. Enlarged and cropped versions of panels I through L are shown in Fig. S1 and explained in the Fig. S1 legend.

Histological analysis of lung sections showed that pICLC treatment results in effective containment of *C. neoformans*, whereas pICLC treatment reduces *C. gattii*-associated pathology without evident immune containment. After 21 days of infection, *C. neoformans* showed extensive pulmonary growth and immune cell recruitment but incomplete containment of *C. neoformans* (Fig. 2A, E, and I). pICLC treatment resulted

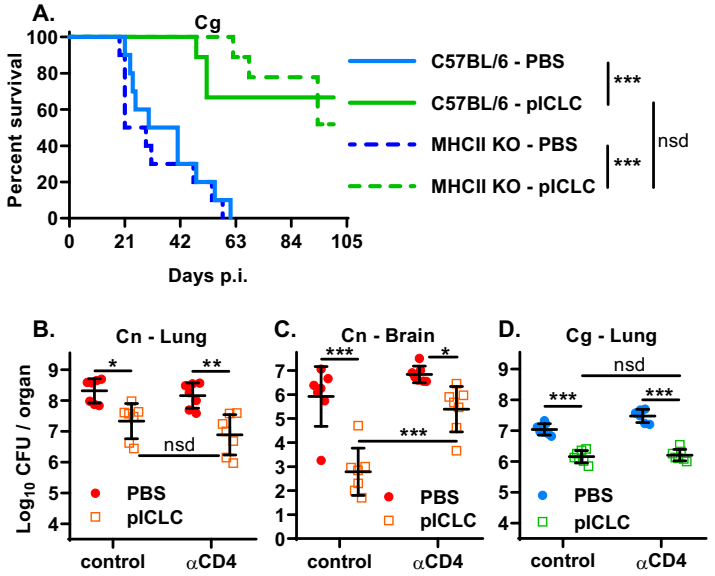

FIG 3 CD4 T-cells are dispensable for pICLC-mediated resistance to *C. gattii*. (A) *C. gattii* (Cg)-infected MHC-II-deficient mice (MHCII KO) and C57BL/6 control mice treated with pICLC or with PBS vehicle control. Data are from 9 or 10 mice per group with 2 independent infections. For panels B to D, mice were depleted of CD4 T cells using anti-CD4 monoclonal antibody and were infected, alongside control mice, with *C. neoformans* (Cn) (B and C) or *C. gattii* (D) and treated with pICLC or PBS vehicle as described previously. Mouse lungs (B and D) and brains (C) were harvested 21 days postinfection, and fungal loads were determined. Data are combined from two independent experiments with 6 or 7 total mice per group.

in markedly better containment of *C. neoformans* yeast within tightly packed lesions ringed by immune cells allowing relatively healthy lung tissue outside the lesions (Fig. 2B, F, and J; see Fig. S1J in the supplemental material). In contrast, *C. gattii* infection resulted in a diffuse yeast distribution within lung air spaces and few recruited immune cells (Fig. 2C, G, and K). *C. gattii* infection resulted in widespread disruption of alveoli (Fig. 2G) and extensive alcian blue- and mucicarmine-positive material in the lung airways (Fig. 2C and K). pICLC treatment of *C. gattii*-infected mice resulted in fewer yeast cells within the lungs and a much more robust recruitment of immune cells. However, most recruited leukocytes were located near airways and not near *C. gattii* cells, leading to incomplete microbial containment (Fig. 2D, H, and L; Fig. S1L). Overall, pICLC treatment reduced the extent of pathological alveolar disruption (Fig. 2G versus Fig. 2H) and airway involvement (Fig. 2C versus Fig. 2D).

pICLC-mediated resistance to *C. gattii* is independent of CD4 T cells. We hypothesized that some factor or factors of HIV/AIDS select against *C. gattii* but not *C. neoformans*. HIV/AIDS is characterized by both elevated t1IFN and depletion of CD4 T cells (9–11), so to model this immune state as well as to determine the role of CD4 T cells in pICLC-mediated *C. gattii* resistance, we examined pICLC-treated CD4 T-cell-depleted animals. In *C. gattii*-infected mice lacking CD4 T cells, due to major histocompatibility complex (MHC) class II genetic deficiency, pICLC treatment resulted in indistinguishable survival between mutant and wild-type mice (Fig. 3A). This contrasts with previous observations in which pICLC-treated CD4 T-cell-deficient mice were susceptible to *C. neoformans* infection (16). To confirm this difference between *C. gattii* and *C. neoformans* infections in another model, we used monoclonal antibody to deplete CD4 T cells. In *C. neoformans*-infected mice, pICLC treatment reduced lung fungal loads in both CD4-depleted and control mice (Fig. 3B). However, CD4 depletion markedly reversed the pICLC-mediated reduction in brain fungal loads (Fig. 3C), consistent with the genetic depletion model (16). In *C. gattii*-infected mice, pICLC treatment similarly reduced lung fungal loads in both CD4-depleted and control mice (Fig. 3D). Thus, both models agree that pICLC-mediated resistance to *C. gattii* was intact in CD4 T-cell-

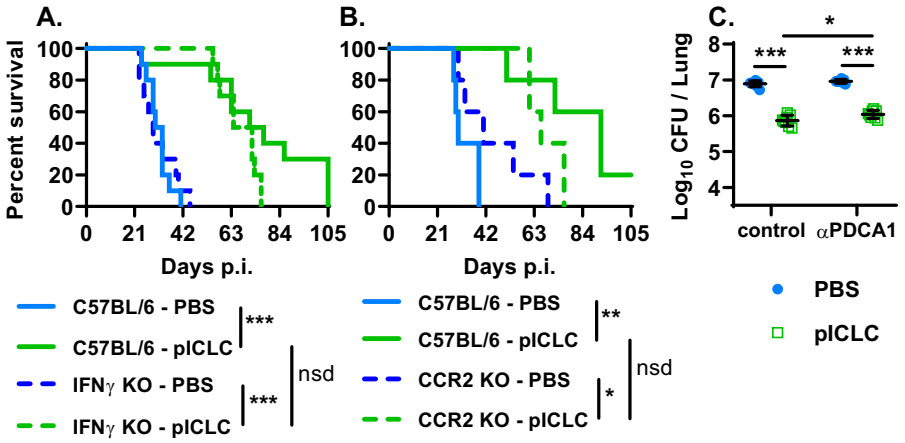

FIG 4 IFN-γ, CCR2, and plasmacytoid dendritic cells are all dispensable for pICLC-mediated resistance to *C. gattii*. (A) IFN-γ-deficient (IFN-γ KO), (B) CCR2-deficient (CCR2 KO), and C57BL/6 control mice were infected with *C. gattii* (Cg) and treated with pICLC or PBS as described previously. Data in panel A are combined from two independent experiments with a total of 10 mice per group. Data in panel B are from one experiment with 5 mice per group. (C) Mice were depleted of plasmacytoid dendritic cells using anti-PDCA1 monoclonal antibody, infected with *C. gattii*, and treated with pICLC or PBS vehicle as described previously. Lung fungal loads 14 days postinfection are shown. Data are combined from two independent experiments with a total of 8 mice per group.

depleted animals, suggesting that CD4 T cells are dispensable for pICLC resistance to *C. gattii* but critical for pICLC resistance to *C. neoformans*.

Neither classical type I immune factors nor pDCs are required for pICLC-mediated resistance. Productive immunity to *C. neoformans* typically flows through the classical immune pathway, where type I T-helper cells secrete IFN-γ, which classically activates recruited myeloid cells to become fungicidal (23, 27, 40). Resistance to *C. neoformans* induced by pICLC was shown here (Fig. 3) and previously (16) to depend on CD4 T cells and IFN-γ, suggesting that pICLC-mediated resistance flows through this classical pathway for cryptococcal immunity. Since CD4 T cells were not a critical component of pICLC-induced resistance to *C. gattii*, our next goal was to determine the mechanisms that do mediate this resistance. While we have shown that CD4 T cells are not critical for pICLC-induced resistance to *C. gattii*, it remained possible that the remaining components of this pathway are activated. IFN-γ is a critical cytokine for activating fungicidal activities in recruited phagocytes, and CCR2-deficient mice do not recruit the monocyte-derived macrophages that can become fungicidal (23). pICLC-mediated resistance to *C. gattii* was intact in IFN-γ-deficient (Fig. 4A) and CCR2-deficient (Fig. 4B) mice. These data suggest that neither IFN-γ nor monocyte-derived CCR2-dependent macrophages are critical for pICLC-mediated resistance to *C. gattii*.

Plasmacytoid dendritic cells (pDCs) can produce large amounts of t1IFN. Also, a recent study suggested that these cells may be relevant in mouse models of cryptococcosis (41). pICLC-treated pDC-depleted mice showed a lung fungal burden that was indistinguishable from that of pICLC-treated nondepleted mice (Fig. 4C), suggesting that pDCs are dispensable for pICLC-mediated resistance. Together these data suggest that the classical anticryptococcal pathway does not mediate pICLC-induced resistance to *C. gattii*.

pICLC-mediated resistance to *C. gattii* is β-2-microglobulin dependent but T-cell, B-cell, and NK cell independent. While investigating immune factors that could underlay pICLC-mediated resistance to *C. gattii*, we considered whether CD8 T cells could be important for resistance. β-2-Microglobulin (B2m)-deficient mice lack surface (MHC-I) and thus lack CD8 T cells and have been used as a model for CD8 T-cell deficiency (42). pICLC-treated B2m-deficient mice showed drastically reduced resistance to *C. gattii* compared to pICLC-treated control mice (Fig. 5A), suggesting that CD8 T cells may mediate pICLC-induced resistance. However, CD8 T-cell antibody depletion

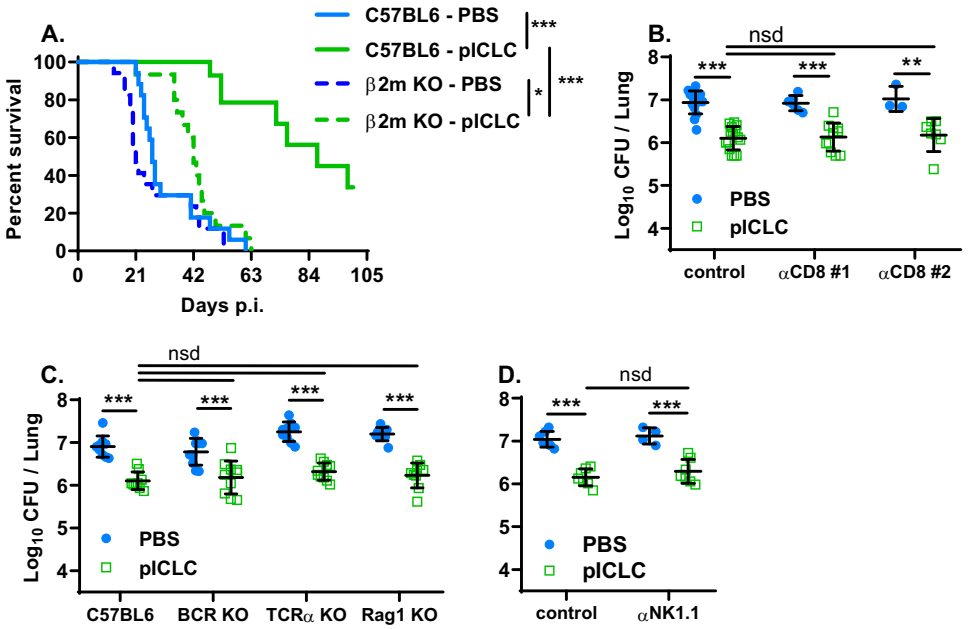

FIG 5 pICLC-induced resistance to Cg is β-2-microglobulin dependent but independent of T, B, and NK cells. (A) β-2-Microglobulin-deficient (B2m KO) and C57BL/6 control mice were infected with *C. gattii* and treated with pICLC or PBS as described previously. Data are combined from three independent experiments with 14 to 17 total mice per group. (B) CD8 T cells were depleted with anti-CD8 monoclonal antibodies (αCD8#1 indicates clone YTS-169.4, and αCD8#2 indicates clone 53-6.72) as described in Materials and Methods, and mice were infected with *C. gattii* and treated with pICLC as described previously. Lung fungal burdens were measured 14 days postinfection, and data are combined from 2 to 3 experiments with $n = 15$ mice per group for the control mice, 6 to 11 mice per group for the anti-CD8#1 group, and 3 to 7 mice for the anti-CD8#2 group. (C) B-cell-receptor-deficient (BCR KO), T-cell-receptor-deficient (TCR KO), Rag1-deficient (Rag1 KO), and C57BL/6 control mice were infected with *C. gattii* and treated with pICLC or PBS as described previously. Lung fungal burdens 14 days postinfection are combined from 2 experiments with $n = 9$ or 10 mice per group. (D) NK cells were depleted with anti-NK1.1 monoclonal antibody, and the mice were infected with *C. gattii* and treated with pICLC. Lung fungal burdens 14 days postinfection are combined from 2 independent experiments with $n = 4$ to 7 mice per group.

in *C. gattii*-infected mice did not alter pICLC-mediated resistance as measured by fungal loads (Fig. 5B). Combined with the results in Fig. 4, these data illustrate that both CD4 and CD8 T cells are dispensable for pICLC-mediated resistance to *C. gattii*. To confirm this point as well as to check for possible CD4-CD8 T-cell redundancy in pICLC resistance (either CD4 or CD8 T cells could be required, but not necessarily both), we examined pICLC resistance to *C. gattii* in T-cell receptor (TCR)-deficient mice, which lack both CD4 and CD8 T cells. TCR-deficient mice showed intact pICLC-mediated reduction in lung fungal burdens compared control mice (Fig. 5C). Overall, these data suggest that while B2m is somehow critical for pICLC-mediated resistance, CD8 (and CD4) T cells are dispensable.

Because B2m is a cofactor for proteins involved in several pathways, B2m-deficent mice have several immunological and biochemical perturbations aside from CD8 T-cell deficiency. B2m is an important cofactor for the neonatal Fc receptor, which recycles IgG from endosomes, preventing IgG degradation and thereby maintaining serum IgG titers (43–45); thus, B2m-deficient mice have perturbed antibody-mediated immunity (46). To test the role of antibody in mediating pICLC-mediated resistance we utilized B-cell receptor (BCR)-deficient mice, which lack B cells and have deficient antibody responses. The pICLC-mediated reductions of *C. gattii* lung fungal burden were similar between BCR-deficient and control animals (Fig. 5C). Thus, T cells and B cells are independently dispensable for pICLC-mediated resistance from *C. gattii*. To rule out any redundancy between these lymphocyte groups, Rag1-deficent mice, which lack both T cells and B cells, were utilized. Again, pICLC-mediated resistance was intact in these *C. gattii*-infected pICLC-treated Rag1-deficent mice (Fig. 5C), confirming that pICLC-mediated resistance is independent of T and B cells. B2m deficiency also leads to

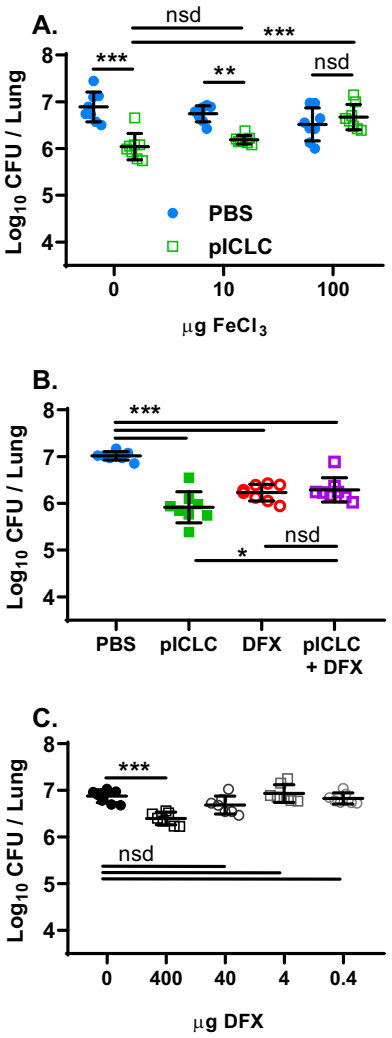

FIG 6 pICLC-induced resistance to *C. gattii* depends on iron limitation. (A) Mice were infected with *C. gattii* and treated with pICLC as previously described and given the indicated doses of iron chloride. (B) C57BL/6 mice were infected with *C. gattii* and treated with pICLC, deferasirox at 400 μg per dose (DFX), or pICLC and DFX. (C) C57BL/6 mice were infected with *C. gattii* and treated with DFX at the indicated doses. All graphs are lung fungal burdens 14 days postinfection with each combined from 2 independent experiments with $n = 7$ or 8 mice per group.

perturbations in NK cell function (47). To test the role of NK cells in pICLC-mediated resistance to *C. gattii*, NK cells were antibody depleted. pICLC-mediated resistance was intact in NK-cell-depleted mice compared to control mice (Fig. 5D), suggesting that NK cells are also dispensable for pICLC-mediated resistance.

pICLC treatment induces iron limitation in mouse lungs. B2m is also a cofactor for an iron regulatory protein, called HFE (high iron Fe), resulting in abnormally elevated iron levels, hemochromatosis, in B2m-deficient mice (48–50). Thus, the dependence of *C. gattii* pICLC-mediated resistance on B2m coupled with the independence of the resistance effect from T cells, B cells, and NK cells suggested the hypothesis that pICLC induces pulmonary iron limitation, which inhibits *C. gattii*. To test this, iron was administered to *C. gattii*-infected control and pICLC-treated animals. Mice administered $FeCl_3$ at 100 μg/dose showed a total loss of pICLC-mediated resistance, as measured by lung *C. gattii* loads (Fig. 6A), implying that iron limitation is critical for pICLC-mediated resistance. Next, iron limitation was exogenously induced by dosing mice with an iron chelator (deferasirox [DFX]). DFX-treated *C. gattii*-infected mice showed similarly reduced fungal loads compared to the pICLC-treated mice (Fig. 6B).

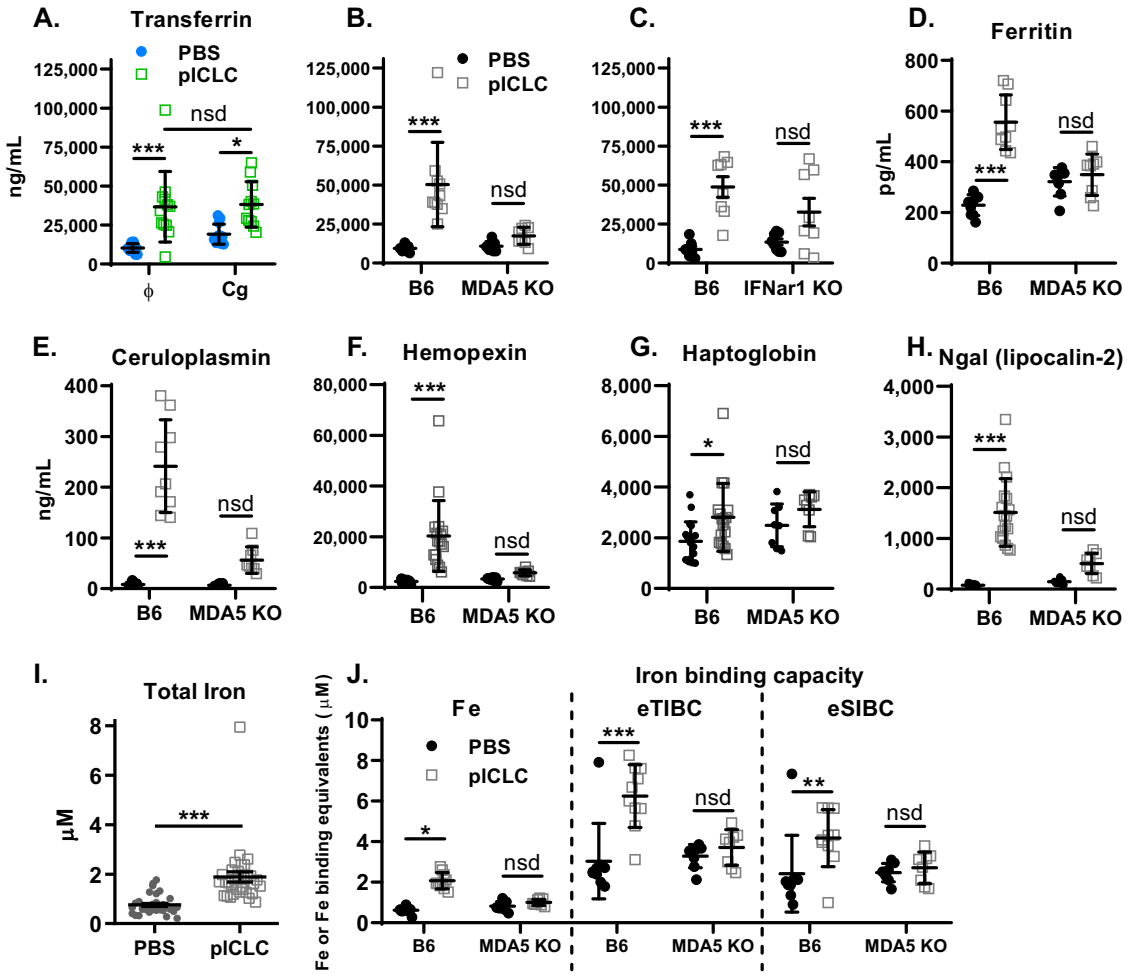

FIG 7 Iron-binding proteins are expressed into the lung air space in response to pICLC. The indicated strains of mice were treated with pICLC or PBS vehicle control, and then after 1 week of treatment, the mice were sacrificed and bronchoalveolar lavage samples were collected for each mouse. The indicated mice in panel A were infected with *C. gattii*, while all other mice were uninfected. Lavage samples were analyzed by ELISA for transferrin (A to C), ferritin (D), ceruloplasmin (E), hemopexin (F), haptoglobin (G), and Ngal/lipocapin-2 (H), and total iron levels were determined by ICP-MS (I) as described in Materials and Methods. For panels A to H, data are from 8 to 18 mice combined from 2 to 4 independent experiments, while for panel I, data are from 33 to 34 mice combined from 7 independent experiments. For panel J, estimated total iron binding capacity (eTIBC) and estimated spare iron binding capacity (eSIBC) were calculated as described in Materials and Methods. For panel J, 9 or 10 mice were analyzed from 2 independent experiments.

DFX-mediated reduction in *C. gattii* fungal loads was dose dependent (Fig. 6C). Importantly, dosing *C. gattii*-infected mice with both pICLC and DFX showed no additional reduction in fungal loads beyond that mediated by pICLC or DFX alone (Fig. 6B), consistent with these treatments functioning via the same pathway. Together, these data show that iron limitation is necessary for pICLC-mediated resistance to *C. gattii* and that direct drug-mediated iron limitation is sufficient to provide similar resistance.

Exogenous induction of t1IFN induces accumulation of iron-related proteins in the lung air space. To investigate the nature of pICLC-induced iron limitation, we measured the concentrations of iron-associated proteins in lung lavage samples from pICLC-treated versus phosphate-buffered saline (PBS) vehicle-treated control mice. pICLC dosing increased levels of transferrin (TfN) in lung lavage samples compared to those in PBS vehicle-treated control mice (Fig. 7A). This pICLC-induced TfN expression was similar in *C. gattii*-infected and uninfected mice, suggesting that the induction of TfN was infection independent and triggered by pICLC alone (Fig. 7A). pICLC dosing of MDA-5-deficient mice did not result in increased TfN (Fig. 7B), confirming that TfN induction is specific to pICLC signaling through MDA-5. Similarly, pICLC dosing of

IFNar1-deficient mice resulted in lung TfN not significantly different from that in untreated mice (Fig. 7C), suggesting that most TfN expression depends on t1IFN signaling. While TfN is the major serum iron-binding protein in mammals, ferritin (Ftn) is the major intracellular iron storage protein and is secreted in some settings (51). Significantly higher levels of Ftn were observed in lavage from pICLC-treated compared to untreated mice (Fig. 7D). This pICLC-increased Ftn expression was also MDA-5 dependent (Fig. 7D). Ceruloplasmin (CP) is a serum ferroxidase protein that facilitates iron loading into TfN (52). pICLC treatment highly induced CP in an MDA-5-dependent manner (Fig. 7E). Hemopexin (Hpx), haptoglobin (Hap), and Ngal/lipocalin-2 are mammalian proteins that sequester iron from heme, hemoglobin, and siderophores, respectively (53). Hpx (Fig. 7F) and Ngal (Fig. 7H) were substantially induced by pICLC, with only a moderate induction of Hap (Fig. 7G), and as with TfN, Ftn, and CP, the induction of these proteins was entirely MDA-5 dependent. Thus, pICLC signaling through MDA-5 induces expression of several iron-scavenging proteins into the lung air space fluids.

If iron restriction is mediated by iron binding, it follows that the iron concentration does not exceed the iron binding capacity of the induced proteins. Inductively coupled plasma mass spectrometry (ICP-MS) measurement of iron concentrations in lung lavage samples showed that pICLC dosing induced a modest increase in iron levels (Fig. 7I) that was specific to MDA-5 signaling (Fig. 7J). However, this modest pICLC-induced increase in iron was significantly less than the MDA-5-dependent pICLC-induced increase in predicted iron binding capacity (Fig. 7J).

Iron-binding proteins inhibit both *Cryptococcus* species *in vitro* but are more potent against *C. gattii*. Since *in vivo* inhibition of *C. gattii* by pICLC requires iron restriction (Fig. 6) and pICLC treatment induces proteins with spare iron binding capacity (Fig. 7), secretion of these proteins may be a potential mediator of the observed *C. gattii* inhibition. Thus, the direct anticryptococcal activities of TfN and Ftn were measured *in vitro*. TfN (Fig. 8A) and Ftn (Fig. 8B) directly inhibited both cryptococcal species, and interestingly, TfN and Ftn were both more potent inhibitors of *C. gattii* than *C. neoformans*. Cryptococcal growth inhibition by 10 μM TfN was reversed with the addition of 40 μM iron with either *C. gattii* or *C. neoformans* (Fig. 8C). Importantly, the addition of 40 μM iron did not appreciably change the growth of *C. gattii* or *C. neoformans* without iron-binding proteins, so this was a specific reversal of TfN-mediated inhibition and not a general growth rate improvement. Similarly, cryptococcal inhibition with 0.1 μM Ftn was reduced by increasing doses of iron with complete reversal of inhibition at 40 μM iron (Fig. 8D). Thus, the iron-binding proteins TfN and Ftn directly inhibit cryptococcal growth via a mechanism that requires iron limitation. Overall, the effective growth inhibition of *C. gattii* by TfN and Ftn is consistent with the induction of these iron-binding proteins underlying the pICLC-mediated resistance to *C. gattii*.

DISCUSSION

The data presented here and in our previous work (16) conclusively show t1IFN induction dramatically reprograms the immune response to more efficiently contain *C. neoformans* in the lungs of mice. Moreover, t1IFN-mediated resistance to *C. neoformans* depends on CD4 T-cells (Fig. 3) (16), but resistance to *C. gattii* does not. These data suggest explanations for several clinical observations of cryptococcosis in AIDS patients. t1IFN-mediated cryptococcal resistance predicts that the early stage of HIV infection, which generates high levels of t1IFN, would render the host resistant to cryptococcal infection by either species. This is consistent with clinical observations that cryptococcosis is not common during early stage HIV, before CD4 T-cell levels are very low (8, 54). Our data also suggest that once CD4 T cells are depleted during advanced AIDS, the t1IFN resistance to *C. neoformans* infection would be lost even if t1IFN levels are maintained. This is consistent with the well-documented susceptibility of individuals with advanced AIDS to *C. neoformans* meningoencephalitis. In contrast to the situation with *C. neoformans*, t1IFN-induced resistance to *C. gattii* does not depend on CD4 T cells, and thus individuals with advanced AIDS would likely remain protected

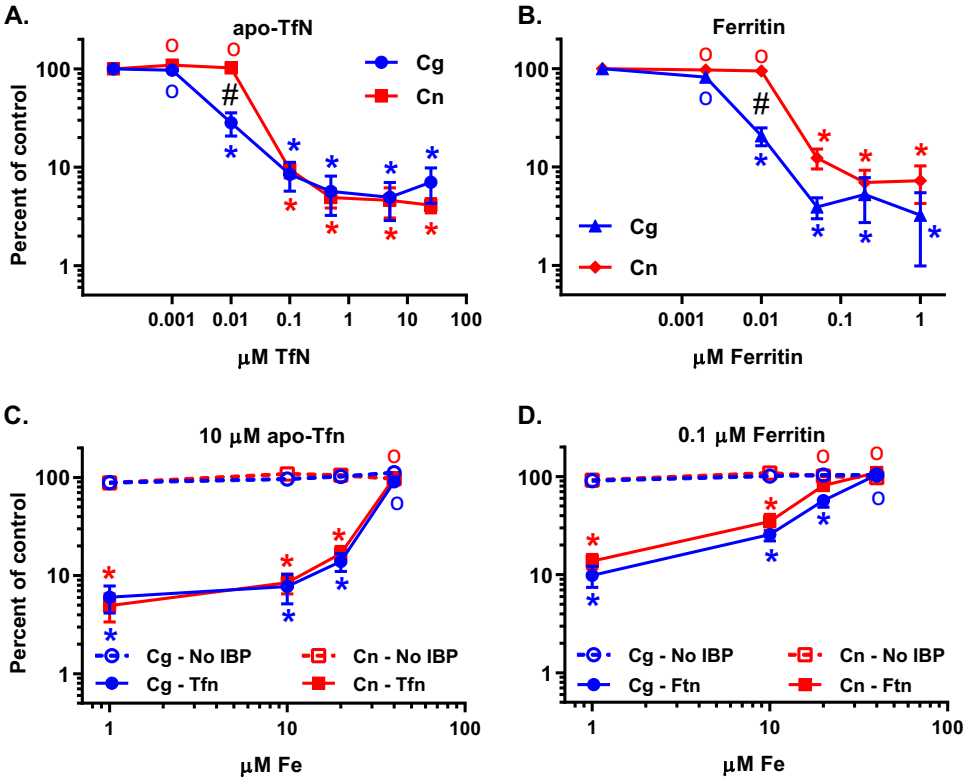

FIG 8 Transferrin and ferritin directly inhibit cryptococcal growth by restricting iron. *In vitro* growth of *Cryptococcus* species was measured after 24 h of incubation with the indicated concentrations of apo-transferrin (A [apo-TfN]) or ferritin (B [Ftn]). For panels A and B, data are normalized to data from wells without TfN or Ftn; these control wells are plotted as the leftmost points for each species. Growth of *C. gattii* and *C. neoformans* was measured in inhibitory concentrations of TfN (C) or Ftn (D) or controls without iron-binding protein ("No IBP") with the indicated concentrations of Fe. In panels C and D, data are normalized to the average of all of the corresponding "No IBP" wells. For panels A to C, data are combined from 3 independent experiments with a total of $n = 12$. For panel D, data are combined from 5 independent experiments with a total of $n = 20$. For all panels, * indicates a statistically significant difference ($P < 0.0005$) and "o" indicates no statistically significant difference ($P > 0.05$) between the indicated data point and the corresponding no-TfN or no-Ftn control. Thus, the indicated points are compared to the far-left point of panel A or B and the corresponding "No IBP" point for panels C and D. # indicates a statistically significant difference ($P < 0.0005$) between *C. gattii* and *C. neoformans* at the indicated concentration of TfN or Ftn. Note that all other *C. gattii* versus *C. neoformans* comparisons in panels A to D were tested and found to be not statistically different.

from *C. gattii*, consistent with the clinical observation that AIDS patients present with *C. gattii* infection much less frequently than *C. neoformans*.

In studies aimed to determine the mechanisms which mediate pICLC-induced resistance to *C. gattii*, we probed several factors usually involved in cryptococcal immunity. The current immunological paradigm for *Cryptococcus* resistance is CD4 T-cell-secreted IFN-γ activates recruited macrophages to become fungicidal (18, 22–26, 31). However, T cells, IFN-γ, and recruited (CCR2) macrophages were dispensable for pICLC-mediated *C. gattii* resistance (Fig. 3 and 5). These data make it unlikely that this classical resistance pathway has an important role in pICLC-mediated resistance to *C. gattii*. Histopathological examination of pICLC-treated *C. gattii*-infected lungs showed that while there was substantial leukocyte recruitment to the lungs, there was little cellular recruitment to the areas of concentrated infection. Instead, leukocytes were concentrated near vasculature and airways—presumably the sites of leukocyte entry into the lungs and pICLC-receptor signaling, respectively (Fig. 2). Additionally, there was little evidence of *C. gattii*-leukocyte contact or *C. gattii* phagocytosis, even in pICLC-treated mice (Fig. S1K and L). This contrasted with pICLC-treated *C. neoformans*-infected lungs, where recruited leukocytes organized to contain *C. neoformans* with evident *C. neoformans*-phagocyte contacts, including phagocytosed yeast (Fig. 2E and F; Fig. S1J).

Together, these data suggest that the pathway of IFN-γ-activating fungicidal macrophages is not a critical mechanism mediating pICLC resistance against *C. gattii*. Furthermore, very little direct immune cell-*C. gattii* engagement was observed (Fig. S1L), so direct cellular immunity seems unlikely, although it cannot be ruled out. This is consistent with soluble factors mediating pICLC-induced *C. gattii* resistance.

These results point to lung air space iron limitation as one such soluble factor that mediates pICLC-induced resistance to *C. gattii*. This conclusion is based on the data presented in Fig. 6 which show addition of iron reverses pICLC *C. gattii* resistance and pharmacological iron limitation phenocopies pICLC resistance. All fungal pathogens (and nearly all microbes) require iron as a critical cofactor for various enzymes. Importantly, *Cryptococcus* requires iron as a critical cofactor for enzymes in the ergosterol synthesis pathway, which is critical for growth (55, 56). Iron availability is sensed as a proxy for the host environment such that low-iron conditions trigger elaboration of the major cryptococcal virulence factors, including capsule, cell wall melanin, and 37°C thermotolerance (57). *Cryptococcus* contains and expresses iron uptake genes involved in siderophore binding, heme, and high-affinity reductive uptake (58). Our data demonstrate pICLC induces host proteins capable of sequestering iron from each of these uptake pathways (Fig. 7). That said, only minor roles have been demonstrated for the heme and siderophore uptake pathways in cryptococcal mouse models, while deletion of any part of the high-affinity reductive pathway substantially reduces virulence (56, 59–62). An important consideration is that almost all published *Cryptococcus* iron acquisition studies utilize *C. neoformans*, and thus *C. gattii* iron uptake in the host has not been characterized and may be substantially different. The cryptococcal high-affinity reductive uptake system requires reduction of ferric (III) to ferrous (II) iron, followed by uptake and reoxidation by a separate complex (58), so free ferrous iron could be vulnerable during this pathway to host proteins. Of note, soluble TfN (63) and Ftn (64) and lactoferrin, a related protein (48), have antimicrobial effects in other systems. While further studies are required to determine the mechanism(s) by which iron-binding proteins inhibit cryptococcal growth, host expression of iron-binding proteins seems likely to interfere with critical iron acquisition.

Iron restriction is a well-established host strategy utilized to limit microbial iron access (53), best characterized during inflammatory extracellular bacterial infection. Systemic inflammatory cytokines trigger signals causing splenic and liver macrophages to retain iron liberated by homeostatic erythrocyte turnover, resulting in a global reduction of circulating iron. If inflammation persists, erythrocyte progenitors cannot accumulate sufficient iron, resulting in anemia. Parallel to this, iron-scavenging acute-phase proteins, including Ftn, Hpx, Hap, and Ngal, are secreted into blood during inflammation. Intracellular bacterial infection triggers an independent response that transports iron out of both the bacterium-containing vacuole and the phagocyte cytosol. Our data suggest a novel system considerably different from these previously characterized iron restriction systems. First, iron restriction in response to t1IFN has not been well characterized. Second, the iron restrictive effect observed here is most likely local to the lungs or perhaps local microenvironments as we were unable to detect any pICLC-mediated changes to serum TfN or iron levels (see Fig. S2 in the supplemental material). Additionally, it is interesting to note that local iron levels did not actually decrease with pICLC treatment (Fig. 7I). This contrasts with the previously characterized systems, which deplete iron from the site of infection. The data presented above suggest that pICLC signaling through MDA-5 induces a set of host factors capable of scavenging free and prosthetic-bound iron in the lung air space fluids. This iron restriction system has potential relevance in a variety of infectious models beyond cryptococcosis.

While exogenous t1IFN induction mediated significant resistance to both species of *Cryptococcus*, the role of endogenous t1IFN during cryptococcal infection seems to depend highly on the strains and conditions used. Our previous study (16), along with two others (65, 66), suggests a host protective role for endogenous t1IFN in *C. neoformans* infection with a possible role in driving productive immunity. In contrast,

a separate study showed a host detrimental role for endogenous t1IFN during *C. neoformans* infection, with t1IFN driving nonproductive immune responses (67). Another group observed that coinfection with *C. gattii* and influenza virus, which induces high levels of t1IFN along with other inflammatory mediators, induced a marked inflammatory lung pathology increase without much change in fungal loads (68). Note that several different *C. neoformans* and mouse strains were used in these studies, perhaps accounting for their contrasting outcomes. In fact, even within this project, we observed substantially superior pIClC-mediated resistance to *C. gattii* compared to *C. neoformans* (Fig. 1). This was especially interesting considering that pIClC induced a robust immune containment (Fig. 2) and the induction of classical anticryptococcal pathways against *C. neoformans* (Fig. 3) (16). One possible explanation for the more robust pIClC-mediated resistance to *C. gattii* than *C. neoformans* is that *C. gattii* is more sensitive to iron-binding protein inhibition (Fig. 7 and 8). While further studies are required to fully understand the differences in pIClC-mediated resistance to *C. gattii* versus *C. neoformans*, the superior pIClC-mediated resistance to *C. gattii* compared to *C. neoformans* and the T-cell dependence of pIClC resistance to *C. neoformans* but not *C. gattii* are both consistent with HIV infection selecting against *C. gattii* in favor of *C. neoformans*.

MATERIALS AND METHODS

***Cryptococcus* strains and culture.** *Cryptococcus neoformans* H99 and *Cryptococcus gattii* R265 were maintained as frozen stocks at −80°C in 20% glycerol. For mouse infection, fresh cultures from stocks were shaken overnight in YPD (yeast extract-peptone-dextrose [MP Biomedicals, Santa Ana, CA]) at 30°C, rinsed, enumerated, and diluted to 5,000 yeast cells per mouse (20 μl per mouse) in sterile PBS.

Mice. Wild-type C57BL/6 mice were purchased from Taconic (Germantown, NY). MDA-5$^{-/-}$, IFNar1$^{-/-}$, MHC-II$^{-/-}$ (C57BL/6NTac-[KO]AbB), $B_2m^{-/-}$, IFN-$\gamma^{-/-}$, BCR$^{-/-}$ (C57BL/10SgSnAi-[KO]uMT), TCR-$\alpha^{-/-}$, RAG1$^{-/-}$, and CCR2$^{-/-}$ mice were purchased under the NIAID Taconic supply agreement. All mice were females of ages 8 to 12 weeks at the start of experiments.

Ethics statement. The Institutional Animal Care and Use Committee of the National Institute of Allergy and Infectious Diseases approved all animal studies (approval no. LCIM-5E). Studies were performed in accordance with the recommendations of the *Guide for the Care and Use of Laboratory Animals* of the National Institutes of Health (69).

Administration of microbes and treatments to mice. *Cryptococcus*, pIClC, iron (ferric) chloride, and DFX were administered by intrapharyngeal aspiration. All treatments started the day of or the day before infection and extended for the duration of each experiment. pIClC (Hiltonol supplied by Oncovir, Inc.) was administered at 5 μg per dose twice per week. Sterile filtered ferric chloride (Sigma-Aldrich) was neutralized with sodium hydroxide and diluted in sterile PBS to the doses indicated and given three times per week. DFX was purchased as ExJade (125 mg deferasirox tablets for oral administration) from Novartis through the NIH veterinary pharmacy. ExJade tablets were resuspended and diluted in sterile PBS and administered three times per week.

Mouse infection studies. Infected mice were observed daily for indications of disease and discomfort. Mice that had progressed to irreversible disease (inability to access food or water, persistent lethargy, or severe neurological symptoms) were euthanized. In some experiments, mice were euthanized at predetermined time points following infection (as indicated in the figures and legends). Lungs and brains were harvested from euthanized mice and homogenized by a probe homogenizer, and fungal loads were determined by dilution plating for CFU.

Histology. Following euthanasia, mouse lungs were inflated with formalin and then removed and formalin fixed. Paraffin embedding, sectioning, and staining were performed by Histoserv, Inc. (Germantown, MD). The alcian blue, periodic acid-Schiff (PAS), mucicarmine, and hematoxylin and eosin stains were used as indicated in the legend to Fig. 2. Stained tissue sections were imaged by color digital camera microscopy using a Zeiss Axio Observer inverted microscope and Zeiss Zen microscope software (Carl Zeiss Microscopy, Jena, Germany) with consistent microscope settings for each magnification. Images were identically scaled, cropped, and resized in Zeiss Zen software.

Monoclonal antibody depletion. All monoclonal antibodies used for depletion studies were purchased from BioXcell (West Lebanon, NH). Anti-CD4 (clone GK1.5) and anti-CD8a antibodies (clones YTS-169.4 and 53-6.72) were intraperitoneally injected (100 μg per dose) on days relative to the day of infection −8, −5, −1, and +1 and twice a week thereafter. Anti-NK1.1 monoclonal antibody (clone PK136) was injected (100 μg per dose) on days −1 and +1 and twice a week thereafter. Anti-PDCA1 antibody (clone BX444) was injected (250 μg per dose) on days −2, −1, and +1 and twice a week thereafter.

Bronchoalveolar lavage of mice. Following euthanasia, lungs were lavaged using 1 ml sterile PBS with EDTA-free protease inhibitor (Roche). For iron measurement experiments, this buffer was pretreated with Chelex-100 resin (Bio-Rad) to remove trace iron and then filter sterilized. Recovery and quality of lavage fluid were assessed, and then lavage fluid was centrifuged, and supernatants were stored frozen for subsequent analysis. Enzyme-linked immunosorbent assays (ELISAs) detecting transferrin, ferritin,

hemopexin, haptoglobin, and Ngal/lipocapin2 were performed using kits from Immunology Consultants Laboratory, Inc. (Portland, OR), and an ELISA for ceruloplasmin from LifeSpan Biosciences, Inc. (Seattle, WA). In Fig. 7J, lavage samples were split, and TfN, Ftn, and total iron were measured (as described below). For these split samples, estimated total iron binding capacity (eTIBC) was calculated by converting the TfN and Ftn mass-per-milliliter ELISA measurements into micromolar using molecular weights (80 kDa for TfN and 480 kDa for Ftn). The molar protein concentrations were then converted to binding capacities by multiplying by the binding capacity of each iron binding complex. (TfN has 2 iron binding sites, whereas Ftn can bind about 4,500 iron ions [53].) These individual binding capacities for individual samples were summed to equal the eTIBC (TfN binding capacity + Ftn binding capacity = eTIBC). Estimated spare iron binding capacity (eSIBC) = eTIBC – total iron concentration measured by ICP-MS (described below).

Iron measurement. Serum iron levels were analyzed by the NIH Department of Laboratory Medicine using the Iron Gen.2 assay on Cobas 501 or 502 analyzers (Roche Diagnostics, Switzerland). In preliminary data, iron levels in lavage samples were below reliable detection limits using this assay, thus requiring more sensitive detection methods.

Mouse lavage iron levels were measured via ICP-MS analysis. All solutions were prepared using ultrapure water (18 MΩ cm^{-1} [Millipore Milli-Q Element, Bedford, MA]). Standards and the internal standard (indium) were prepared by serial dilution from 1,000-mg $liter^{-1}$ stock solutions (Inorganic Ventures) in 2% nitric acid (Fisher Scientific). All plasticware was preleached with 5% nitric acid for at least 24 h. Samples and standards were diluted 1:5 with 2% nitric acid containing 50 ppb indium. ICP-MS analysis was performed with a Thermo iCAP Q running in kinetic energy discrimination collision cell mode, a PFA microflow nebulizer (Elemental Scientific, Omaha, NE), and a cyclonic spray chamber. Samples were measured in triplicate, and all calibration curves exceeded $R^2 \geq 0.999$.

***In vitro* inhibition assays.** Experiments and precultures were performed in sterile RPMI 1640 medium without L-glutamine (Quality Biological, Gaithersburg, MD) containing 165 mM MOPS (morpholinepropanesulfonic acid [Sigma-Aldrich]) at pH 7.0. Fresh cultures from frozen stocks were shaken overnight in RPMI at 37°C and 5% CO_2, rinsed, enumerated, and diluted in RPMI-MOPS. Ferritin from equine spleen (Sigma-Aldrich), human apo-transferrin (Sigma-Aldrich), and/or iron (EMD Millipore), and *C. neoformans* or *C. gattii* (final concentration of 80,000 per ml) in RPMI-MOPS with 1 μM iron were arrayed in a 2-ml-deep-well plate in a final volume of 0.4 ml/well. The culture plate was sealed with a gas-permeable membrane (USA Scientific, FL) and shaken at 37°C and 5% CO_2 for 24 h. Fungal growth and inhibition were determined by dilution plating for CFU. Data were normalized to a percentage of the control by the following formula: 100 × (experimental no. of CFU)/(control no. of CFU). The control conditions used to normalize each experiment are indicated in the legend to Fig. 8.

Statistical analysis. Experimental significance tests were performed as indicated using GraphPad Prism (San Diego, CA). Briefly, mouse mortality was compared pairwise by Mantel-Cox log rank test. Log_{10}-transformed fungal loads were compared by analysis of variance (ANOVA). Subsequent multiple comparisons were done with pairwise Student's *t* tests with Tukey's correction. Each graphed point represents one mouse with indicated plotted means and error bars representing the standard error of the mean (SEM). For all comparison testing, * indicates $P < 0.05$, ** indicates $P < 0.005$, *** indicates $P < 0.0005$, and "nsd" indicates not statistically different ($P > 0.05$).

SUPPLEMENTAL MATERIAL

Supplemental material for this article may be found at https://doi.org/10.1128/mBio.00799-19.

FIG S1, PDF file, 1.8 MB.

FIG S2, PDF file, 0.7 MB.

ACKNOWLEDGMENTS

We wish to acknowledge the NIH Department of Laboratory Medicine for their generous assistance with the measurement of serum iron levels.

This work was supported by a research fund from the intramural program of the National Institute of Allergy and Infectious Diseases, National Institutes of Health. The authors declare no competing financial interests.

REFERENCES

1. Kwon-Chung KJ, Fraser JA, Doering TL, Wang Z, Janbon G, Idnurm A, Bahn YS. 2014. Cryptococcus neoformans and Cryptococcus gattii, the etiologic agents of cryptococcosis. Cold Spring Harb Perspect Med 4:a019760. https://doi.org/10.1101/cshperspect.a019760.
2. Emmons CW. 1955. Saprophytic sources of Cryptococcus neoformans associated with the pigeon (Columba livia). Am J Hyg 62:227–232.
3. Bauwens L, Swinne D, De Vroey C, De Meurichy W. 1986. Isolation of Cryptococcus neoformans var. neoformans in the aviaries of the Antwerp Zoological Gardens. Mykosen 29:291–294.
4. Ellis DH, Pfeiffer TJ. 1990. Natural habitat of Cryptococcus neoformans var. gattii. J Clin Microbiol 28:1642–1644.
5. Kidd SE, Chow Y, Mak S, Bach PJ, Chen H, Hingston AO, Kronstad JW, Bartlett KH. 2007. Characterization of environmental sources of the human and animal pathogen Cryptococcus gattii in British Columbia, Canada, and the Pacific Northwest of the United States. Appl Environ Microbiol 73:1433–1443. https://doi.org/10.1128/AEM.01330-06.
6. Meyer W, Gilgado F, Ngamskulrungroj P, Trilles L, Hagen F, Castaneda E, Boekhout T. 2011. Molecular typing of the Cryptococcus neoformans/Cryptococcus gattii species complex, p 327–357. *In* Heitman J, Kozel TR,

Kwon-Chung KJ, Perfect JR, Casadevall A (ed), Cryptococcus: from human pathogen to model yeast. ASM Press, Washington, DC.
7. Ghosn J, Taiwo B, Seedat S, Autran B, Katlama C. 2018. HIV. Lancet 392:685–697. https://doi.org/10.1016/S0140-6736(18)31311-4.
8. Rajasingham R, Smith RM, Park BJ, Jarvis JN, Govender NP, Chiller TM, Denning DW, Loyse A, Boulware DR. 2017. Global burden of disease of HIV-associated cryptococcal meningitis: an updated analysis. Lancet Infect Dis 17:873–881. https://doi.org/10.1016/S1473-3099(17)30243-8.
9. Lopez C, Fitzgerald PA, Siegal FP. 1983. Severe acquired immune deficiency syndrome in male homosexuals: diminished capacity to make interferon-alpha in vitro associated with severe opportunistic infections. J Infect Dis 148:962–966. https://doi.org/10.1093/infdis/148.6.962.
10. Sandler NG, Bosinger SE, Estes JD, Zhu RT, Tharp GK, Boritz E, Levin D, Wijeyesinghe S, Makamdop KN, del Prete GQ, Hill BJ, Timmer JK, Reiss E, Yarden G, Darko S, Contijoch E, Todd JP, Silvestri G, Nason M, Norgren RB, Jr, Keele BF, Rao S, Langer JA, Lifson JD, Schreiber G, Douek DC. 2014. Type I interferon responses in rhesus macaques prevent SIV infection and slow disease progression. Nature 511:601–605. https://doi.org/10.1038/nature13554.
11. Poli G, Orenstein JM, Kinter A, Folks TM, Fauci AS. 1989. Interferon-alpha but not AZT suppresses HIV expression in chronically infected cell lines. Science 244:575–577. https://doi.org/10.1126/science.2470148.
12. Pestka S, Krause CD, Walter MR. 2004. Interferons, interferon-like cytokines, and their receptors. Immunol Rev 202:8–32. https://doi.org/10.1111/j.0105-2896.2004.00204.x.
13. Pestka S, Langer JA, Zoon KC, Samuel CE. 1987. Interferons and their actions. Annu Rev Biochem 56:727–777. https://doi.org/10.1146/annurev.bi.56.070187.003455.
14. McNab F, Mayer-Barber K, Sher A, Wack A, O'Garra A. 2015. Type I interferons in infectious disease. Nat Rev Immunol 15:87–103. https://doi.org/10.1038/nri3787.
15. Seyedmousavi S, Davis MJ, Sugui JA, Pinkhasov T, Moyer S, Salazar AM, Chang YC, Kwon-Chung KJ. 2018. Exogenous stimulation of type I interferon protects mice with chronic granulomatous disease from aspergillosis through early recruitment of host-protective neutrophils into the lung. mBio 9:e00422-18. https://doi.org/10.1128/mBio.00422-18.
16. Sionov E, Mayer-Barber KD, Chang YC, Kauffman KD, Eckhaus MA, Salazar AM, Barber DL, Kwon-Chung KJ. 2015. Type I IFN induction via poly-ICLC protects mice against cryptococcosis. PLoS Pathog 11:e1005040. https://doi.org/10.1371/journal.ppat.1005040.
17. Schneider WM, Chevillotte MD, Rice CM. 2014. Interferon-stimulated genes: a complex web of host defenses. Annu Rev Immunol 32:513–545. https://doi.org/10.1146/annurev-immunol-032713-120231.
18. Arora S, Hernandez Y, Erb-Downward JR, McDonald RA, Toews GB, Huffnagle GB. 2005. Role of IFN-gamma in regulating T2 immunity and the development of alternatively activated macrophages during allergic bronchopulmonary mycosis. J Immunol 174:6346–6356. https://doi.org/10.4049/jimmunol.174.10.6346.
19. Jain AV, Zhang Y, Fields WB, McNamara DA, Choe MY, Chen GH, Erb-Downward J, Osterholzer JJ, Toews GB, Huffnagle GB, Olszewski MA. 2009. Th2 but not Th1 immune bias results in altered lung functions in a murine model of pulmonary Cryptococcus neoformans infection. Infect Immun 77:5389–5399. https://doi.org/10.1128/IAI.00809-09.
20. Kawakami K, Tohyama M, Qifeng X, Saito A. 1997. Expression of cytokines and inducible nitric oxide synthase mRNA in the lungs of mice infected with Cryptococcus neoformans: effects of interleukin-12. Infect Immun 65:1307–1312.
21. Almeida GM, Andrade RM, Bento CA. 2001. The capsular polysaccharides of Cryptococcus neoformans activate normal CD4(+) T cells in a dominant Th2 pattern. J Immunol 167:5845–5851. https://doi.org/10.4049/jimmunol.167.10.5845.
22. Wormley FL, Jr, Perfect JR, Steele C, Cox GM. 2007. Protection against cryptococcosis by using a murine gamma interferon-producing Cryptococcus neoformans strain. Infect Immun 75:1453–1462. https://doi.org/10.1128/IAI.00274-06.
23. Osterholzer JJ, Chen GH, Olszewski MA, Zhang YM, Curtis JL, Huffnagle GB, Toews GB. 2011. Chemokine receptor 2-mediated accumulation of fungicidal exudate macrophages in mice that clear cryptococcal lung infection. Am J Pathol 178:198–211. https://doi.org/10.1016/j.ajpath.2010.11.006.
24. Flesch IE, Schwamberger G, Kaufmann SH. 1989. Fungicidal activity of IFN-gamma-activated macrophages. Extracellular killing of Cryptococcus neoformans. J Immunol 142:3219–3224.
25. Mody CH, Tyler CL, Sitrin RG, Jackson C, Toews GB. 1991. Interferon-gamma activates rat alveolar macrophages for anticryptococcal activity. Am J Respir Cell Mol Biol 5:19–26. https://doi.org/10.1165/ajrcmb/5.1.19.
26. Kawakami K, Kohno S, Kadota J, Tohyama M, Teruya K, Kudeken N, Saito A, Hara K. 1995. T cell-dependent activation of macrophages and enhancement of their phagocytic activity in the lungs of mice inoculated with heat-killed Cryptococcus neoformans: involvement of IFN-gamma and its protective effect against cryptococcal infection. Microbiol Immunol 39:135–143. https://doi.org/10.1111/j.1348-0421.1995.tb02180.x.
27. Davis MJ, Tsang TM, Qiu Y, Dayrit JK, Freij JB, Huffnagle GB, Olszewski MA. 2013. Macrophage M1/M2 polarization dynamically adapts to changes in cytokine microenvironments in Cryptococcus neoformans infection. mBio 4:e00264. https://doi.org/10.1128/mBio.00264-13.
28. Davis MJ, Eastman AJ, Qiu Y, Gregorka B, Kozel TR, Osterholzer JJ, Curtis JL, Swanson JA, Olszewski MA. 2015. Cryptococcus neoformans-induced macrophage lysosome damage crucially contributes to fungal virulence. J Immunol 194:2219–2231. https://doi.org/10.4049/jimmunol.1402376.
29. Fu MS, Coelho C, De Leon-Rodriguez CM, Rossi DCP, Camacho E, Jung EH, Kulkarni M, Casadevall A. 2018. Cryptococcus neoformans urease affects the outcome of intracellular pathogenesis by modulating phagolysosomal pH. PLoS Pathog 14:e1007144. https://doi.org/10.1371/journal.ppat.1007144.
30. De Leon-Rodriguez CM, Rossi DCP, Fu MS, Dragotakes Q, Coelho C, Guerrero Ros I, Caballero B, Nolan SJ, Casadevall A. 2018. The outcome of the Cryptococcus neoformans-macrophage interaction depends on phagolysosomal membrane integrity. J Immunol 201:583–603. https://doi.org/10.4049/jimmunol.1700958.
31. Voelz K, Lammas DA, May RC. 2009. Cytokine signaling regulates the outcome of intracellular macrophage parasitism by Cryptococcus neoformans. Infect Immun 77:3450–3457. https://doi.org/10.1128/IAI.00297-09.
32. Smith LM, Dixon EF, May RC. 2015. The fungal pathogen Cryptococcus neoformans manipulates macrophage phagosome maturation. Cell Microbiol 17:702–713. https://doi.org/10.1111/cmi.12394.
33. Johnston SA, May RC. 2013. Cryptococcus interactions with macrophages: evasion and manipulation of the phagosome by a fungal pathogen. Cell Microbiol 15:403–411. https://doi.org/10.1111/cmi.12067.
34. Schulze B, Piehler D, Eschke M, von Buttlar H, Kohler G, Sparwasser T, Alber G. 2014. CD4(+) FoxP3(+) regulatory T cells suppress fatal T helper 2 cell immunity during pulmonary fungal infection. Eur J Immunol 44:3596–3604. https://doi.org/10.1002/eji.201444963.
35. Wiesner DL, Specht CA, Lee CK, Smith KD, Mukaremera L, Lee ST, Lee CG, Elias JA, Nielsen JN, Boulware DR, Bohjanen PR, Jenkins MK, Levitz SM, Nielsen K. 2015. Chitin recognition via chitotriosidase promotes pathologic type-2 helper T cell responses to cryptococcal infection. PLoS Pathog 11:e1004701. https://doi.org/10.1371/journal.ppat.1004701.
36. Wiesner DL, Smith KD, Kotov DI, Nielsen JN, Bohjanen PR, Nielsen K. 2016. Regulatory T cell induction and retention in the lungs drives suppression of detrimental type 2 Th cells during pulmonary cryptococcal infection. J Immunol 196:365–374. https://doi.org/10.4049/jimmunol.1501871.
37. Stenzel W, Muller U, Kohler G, Heppner FL, Blessing M, McKenzie AN, Brombacher F, Alber G. 2009. IL-4/IL-13-dependent alternative activation of macrophages but not microglial cells is associated with uncontrolled cerebral cryptococcosis. Am J Pathol 174:486–496. https://doi.org/10.2353/ajpath.2009.080598.
38. Heung LJ, Hohl TM. 2019. Inflammatory monocytes are detrimental to the host immune response during acute infection with Cryptococcus neoformans. PLoS Pathog 15:e1007627. https://doi.org/10.1371/journal.ppat.1007627.
39. Wozniak KL, Hardison S, Olszewski M, Wormley FL, Jr. 2012. Induction of protective immunity against cryptococcosis. Mycopathologia 173:387–394. https://doi.org/10.1007/s11046-011-9505-8.
40. Olszewski MA, Zhang Y, Huffnagle GB. 2010. Mechanisms of cryptococcal virulence and persistence. Future Microbiol 5:1269–1288. https://doi.org/10.2217/fmb.10.93.
41. Hole CR, Leopold Wager CM, Mendiola AS, Wozniak KL, Campuzano A, Lin X, Wormley FL, Jr. 2016. Antifungal activity of plasmacytoid dendritic cells against Cryptococcus neoformans in vitro requires expression of Dectin-3 (CLEC4D) and reactive oxygen species. Infect Immun 84:2493–2504. https://doi.org/10.1128/IAI.00103-16.
42. Zijlstra M, Bix M, Simister NE, Loring JM, Raulet DH, Jaenisch R. 1990. Beta 2-microglobulin deficient mice lack CD4-8+ cytolytic T cells. Nature 344:742–746. https://doi.org/10.1038/344742a0.
43. Israel EJ, Wilsker DF, Hayes KC, Schoenfeld D, Simister NE. 1996. In-

creased clearance of IgG in mice that lack beta 2-microglobulin: possible protective role of FcRn. Immunology 89:573–578. https://doi.org/10.1046/j.1365-2567.1996.d01-775.x.
44. Israel EJ, Patel VK, Taylor SF, Marshak-Rothstein A, Simister NE. 1995. Requirement for a beta 2-microglobulin-associated Fc receptor for acquisition of maternal IgG by fetal and neonatal mice. J Immunol 154:6246–6251.
45. Ghetie V, Hubbard JG, Kim JK, Tsen MF, Lee Y, Ward ES. 1996. Abnormally short serum half-lives of IgG in beta 2-microglobulin-deficient mice. Eur J Immunol 26:690–696. https://doi.org/10.1002/eji.1830260327.
46. Christianson GJ, Brooks W, Vekasi S, Manolfi EA, Niles J, Roopenian SL, Roths JB, Rothlein R, Roopenian DC. 1997. Beta 2-microglobulin-deficient mice are protected from hypergammaglobulinemia and have defective antibody responses because of increased IgG catabolism. J Immunol 159:4781–4792.
47. Denkers EY, Gazzinelli RT, Martin D, Sher A. 1993. Emergence of NK1.1+ cells as effectors of IFN-gamma dependent immunity to Toxoplasma gondii in MHC class I-deficient mice. J Exp Med 178:1465–1472. https://doi.org/10.1084/jem.178.5.1465.
48. Schaible UE, Collins HL, Priem F, Kaufmann SH. 2002. Correction of the iron overload defect in beta-2-microglobulin knockout mice by lactoferrin abolishes their increased susceptibility to tuberculosis. J Exp Med 196:1507–1513. https://doi.org/10.1084/jem.20020897.
49. Enns CA. 2001. Pumping iron: the strange partnership of the hemochromatosis protein, a class I MHC homolog, with the transferrin receptor. Traffic 2:167–174. https://doi.org/10.1034/j.1600-0854.2001.020303.x.
50. Barton JC, Edwards CQ, Acton RT. 2015. HFE gene: structure, function, mutations, and associated iron abnormalities. Gene 574:179–192. https://doi.org/10.1016/j.gene.2015.10.009.
51. Korolnek T, Hamza I. 2015. Macrophages and iron trafficking at the birth and death of red cells. Blood 125:2893–2897. https://doi.org/10.1182/blood-2014-12-567776.
52. Linder MC. 2016. Ceruloplasmin and other copper binding components of blood plasma and their functions: an update. Metallomics 8:887–905. https://doi.org/10.1039/c6mt00103c.
53. Soares MP, Weiss G. 2015. The Iron age of host-microbe interactions. EMBO Rep 16:1482–1500. https://doi.org/10.15252/embr.201540558.
54. Tugume L, Rhein J, Hullsiek KH, Mpoza E, Kiggundu R, Ssebambulidde K, Schutz C, Taseera K, Williams DA, Abassi M, Muzoora C, Musubire AK, Meintjes G, Meya DB, Boulware DR, Coat teams A-C. 2019. HIV-associated cryptococcal meningitis occurring at relatively higher CD4 counts. J Infect Dis 219:877–883. https://doi.org/10.1093/infdis/jiy602.
55. Crisp RJ, Pollington A, Galea C, Jaron S, Yamaguchi-Iwai Y, Kaplan J. 2003. Inhibition of heme biosynthesis prevents transcription of iron uptake genes in yeast. J Biol Chem 278:45499–45506. https://doi.org/10.1074/jbc.M307229200.
56. Jung WH, Hu G, Kuo W, Kronstad JW. 2009. Role of ferroxidases in iron uptake and virulence of Cryptococcus neoformans. Eukaryot Cell 8:1511–1520. https://doi.org/10.1128/EC.00166-09.
57. Jung WH, Sham A, White R, Kronstad JW. 2006. Iron regulation of the major virulence factors in the AIDS-associated pathogen Cryptococcus neoformans. PLoS Biol 4:e410. https://doi.org/10.1371/journal.pbio.0040410.
58. Bairwa G, Hee Jung W, Kronstad JW. 2017. Iron acquisition in fungal pathogens of humans. Metallomics 9:215–227. https://doi.org/10.1039/c6mt00301j.
59. Cadieux B, Lian T, Hu G, Wang J, Biondo C, Teti G, Liu V, Murphy ME, Creagh AL, Kronstad JW. 2013. The mannoprotein Cig1 supports iron acquisition from heme and virulence in the pathogenic fungus Cryptococcus neoformans. J Infect Dis 207:1339–1347. https://doi.org/10.1093/infdis/jit029.
60. Saikia S, Oliveira D, Hu G, Kronstad J. 2014. Role of ferric reductases in iron acquisition and virulence in the fungal pathogen Cryptococcus neoformans. Infect Immun 82:839–850. https://doi.org/10.1128/IAI.01357-13.
61. Jung WH, Sham A, Lian T, Singh A, Kosman DJ, Kronstad JW. 2008. Iron source preference and regulation of iron uptake in Cryptococcus neoformans. PLoS Pathog 4:e45. https://doi.org/10.1371/journal.ppat.0040045.
62. Tangen KL, Jung WH, Sham AP, Lian T, Kronstad JW. 2007. The iron- and cAMP-regulated gene SIT1 influences ferrioxamine B utilization, melanization and cell wall structure in Cryptococcus neoformans. Microbiology 153:29–41. https://doi.org/10.1099/mic.0.2006/000927-0.
63. Bruhn KW, Spellberg B. 2015. Transferrin-mediated iron sequestration as a novel therapy for bacterial and fungal infections. Curr Opin Microbiol 27:57–61. https://doi.org/10.1016/j.mib.2015.07.005.
64. Lipiński P, Jarzabek Z, Broniek S, Zagulski T. 1991. Protective effect of tissue ferritins in experimental Escherichia coli infection of mice in vivo. Int J Exp Pathol 72:623–630.
65. Biondo C, Midiri A, Gambuzza M, Gerace E, Falduto M, Galbo R, Bellantoni A, Beninati C, Teti G, Leanderson T, Mancuso G. 2008. IFN-alpha/beta signaling is required for polarization of cytokine responses toward a protective type 1 pattern during experimental cryptococcosis. J Immunol 181:566–573. https://doi.org/10.4049/jimmunol.181.1.566.
66. Qin HJ, Feng QM, Fang Y, Shen L. 2014. Type-I interferon secretion in the acute phase promotes Cryptococcus neoformans infection-induced Th17 cell polarization in vitro. Exp Ther Med 7:869–872. https://doi.org/10.3892/etm.2014.1517.
67. Sato K, Yamamoto H, Nomura T, Matsumoto I, Miyasaka T, Zong T, Kanno E, Uno K, Ishii K, Kawakami K. 2015. Cryptococcus neoformans infection in mice lacking type I interferon signaling leads to increased fungal clearance and IL-4-dependent mucin production in the lungs. PLoS One 10:e0138291. https://doi.org/10.1371/journal.pone.0138291.
68. Oliveira LVN, Costa MC, Magalhaes TFF, Bastos RW, Santos PC, Carneiro HCS, Ribeiro NQ, Ferreira GF, Ribeiro LS, Goncalves APF, Fagundes CT, Pascoal-Xavier MA, Djordjevic JT, Sorrell TC, Souza DG, Machado AMV, Santos DA. 2017. Influenza A virus as a predisposing factor for cryptococcosis. Front Cell Infect Microbiol 7:419. https://doi.org/10.3389/fcimb.2017.00419.
69. National Research Council. 2011. Guide for the care and use of laboratory animals, 8th ed. National Academies Press, Washington, DC.